Thai Environmental Engineering Journal Vol. 36 No. 1 (2022) : 71-87
www.eeat.or.th

Adjusting Ventilation for Heat Control in an Industrial Building Using Computational Fluid Dynamics: Case Study of a Heat Treatment Plant in Automobile Industry

Kritana Prueksakorn[1], Phatra Samerwong[1], Thunyapat Sattraburut[1], Hyunchul Ha[2], Kwangseog Ahn[3] and Taehyeung Kim[4*]

[1]Faculty of Environment and Resource Studies,
Mahidol University, Nakhon Phathom 73170, Thailand
[2]Ventech Corp., Changwon, 641773, South Korea
[3]Department of Occupational & Environmental Safety & Health, University of Wisconsin-Whitewater, Hyland Hall 3501, 800 West Main Street, Whitewater, WI 53190, USA
[4]Department of Environmental Engineering,
Changwon National University, Changwon, 641773, South Korea
[*]E-mail : thkim@changwon.ac.kr

Abstract

Heat strain is a serious health issue in many manufacturing industries, including steel plants, foundries, and automobile industries. This research attempts to control the high temperatures in a heat treatment plant of automobile industry whose existing ventilation methods were insufficient to address the heat-related problems. Preliminary studies were carried out to determine the existing temperatures and air velocities, the effectiveness of the ventilation measures and the problems associated with the heat processes. The obtained data were fed into a computational fluid dynamic (CFD) model with initial and boundary conditions, used to predict the temperature and airflow inside the building. Five additional building models were created, each adding different thermal control and ventilation measures to the initial configuration. Based on the simulations from CFD, a model with windows, ventilators, enclosures, and jet fans was selected as the best case. This ventilation system was then physically installed in the building. The performance of the real system was measured and compared to the predicted values. A good correlation was found between the numerical simulation and the experimental results; the temperature differences between the values at 1.5 m, 3 m and 4.5 m above the ground were 1.8%, 2.7% and 3.3%, respectively. The final ventilation solution was able to decrease the average temperature by 5.3°C and increase the average air velocity by 1.5 m/s. This study demonstrates how numerical modeling and building ventilation solutions can be effectively used to solve the problem of high temperatures in an indoor industrial environment.

Keywords : Computational fluid dynamic; Heat stress; Heat ventilation; Industrial heat control; Jet fan ventilation

Introduction

Heat treatment is a principal manufacturing process that plays an important role in the production of automotive components and regulates the properties of the final product [1-3]. Automotive production generally uses steel, iron, aluminum, plastics, rubber, and glasses as raw materials. Assembling a product from these raw materials requires different types of heat treatments, such as annealing, normalizing, quenching, and tempering. Heat treatment improves the properties of metallic components to achieve the required strength, hardness and durability [4-6]. This makes heat treatment essential for the automotive industry. Heat treatment also generates considerable heat causing a hot and unhealthy industrial environment. Workers working near process-related heat in manufactures such as steel mills, foundries, and automotive plants are at high risk of heat stress [7, 8]. Acute exposure to extreme heat over short periods of time leads to heat stroke, exhaustion, collapse, heat rash, fatigue, and can even lead to death. Long-term exposure leads to cardiovascular disease, mental health problems, and kidney disease [9-11]. It is necessary to protect workers from heat exposure, which can be achieved through engineered safety measures such as insulation, baffles, partitions, personal protective equipment, and ventilation [12].

Recently, jet fans have been widely used to extract polluted air in parking garages and tunnels [13, 14]. In a jet ventilation system, a fan draws in a small amount of air and discharges it at a very high velocity, pushing the polluted air in front of it while drawing in air from the surrounding area. This moves the air long distances without the need to use ducts and requires less installation space due to the high speed of air movement [15]. There is an abundance of research on the use of jet fans in tunnels [16, 17] and parking garages [18-20], but almost none on industrial applications. CFD is a useful tool for predicting air movement in ventilated spaces to determine spatial temperature variations [21], and has been used in engineering for ventilation system design [22]. CFD has been successfully used for a wide range of building applications in the design and evaluation of indoor air flow, thermal comfort, smoke conditions, etc. [23-25]. CFD models have been used for indoor air quality analysis of various building environments including offices, residential buildings, stadiums, historical settlements, etc. [26-29]. Nevertheless, there is still a lack of application in the analysis of heat reduction ventilation in industrial buildings.

The purpose of this study is to adjust the ventilation of an existing building used for heat treatment of automotive parts to reduce the temperature to a comfortable range. The ventilation adjustments are first simulated using CFD and the most favorable case is selected for implementation in the real building. The study focuses on measuring the indoor temperature and velocity, validating CFD model for the existing conditions, CFD simulation of the upgraded building with different ventilation adjustments, and finally comparing the indoor temperature between the best suitable case from the CFD simulation and the implementation in the existing building.

Methods

Description of the Building

The building has dimensions of L **x** W **x** H = 120 m **x** 84 m **x** 12 m and consists of heat sources composed of 5 heat processes. Heat processes 1, 2 and 3 consist of a drying oven, an input chamber, a preheating chamber, a brazing chamber, a cooling chamber and an output. The car parts are transported from each process starting from the drying oven through the exit. Each unit has an individual local exhaust system to extract and remove smoke generated during the heat treatment process [30]. Heat process 4 is a heating oven and heat process 5 is used as a high temperature process to remove oil products. Currently, the building has 6 doors (D1-D6) for access to the interior of the building that also provide natural ventilation, 2 roof monitors for stack ventilation, 10 vents and 28 roof fans that also contribute to the ventilation of the building. The schematic diagram of the external and internal features of the building can be seen in Figure 1.

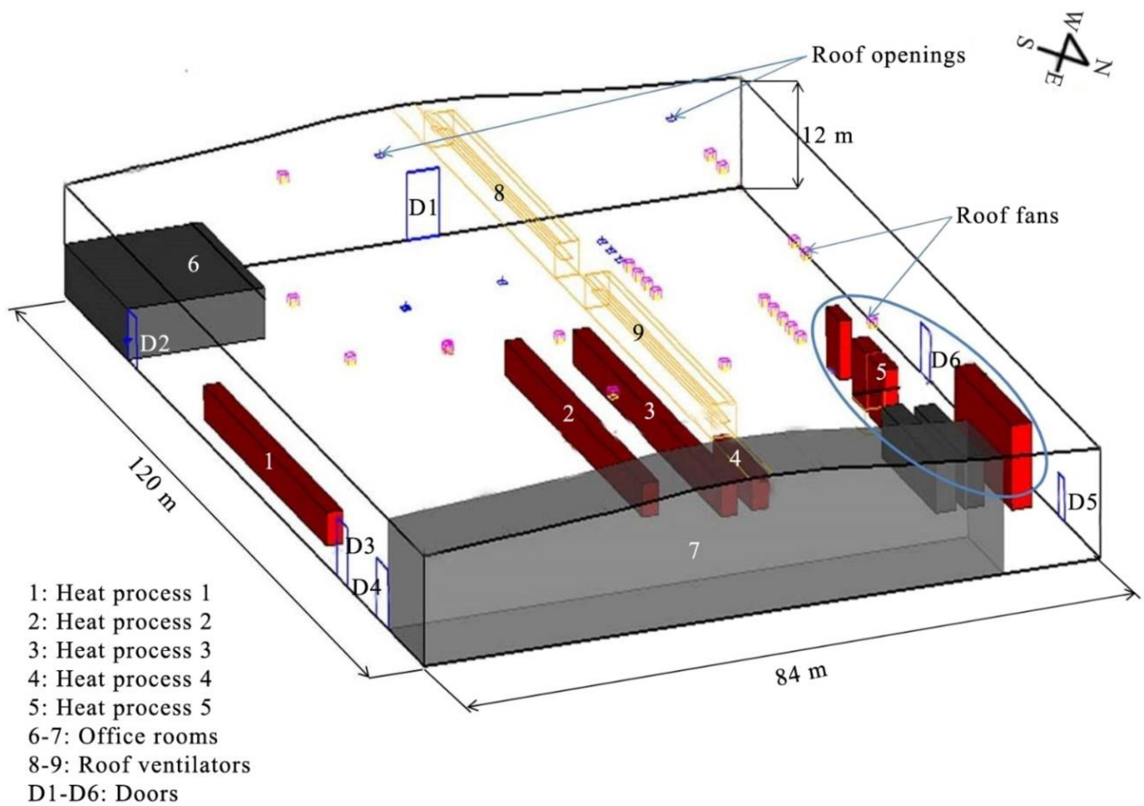

Figure 1 Diagram of the case study building.

Measurements

Temperature

The external surface temperature of the heat treatment equipment was measured using a thermal imaging camera [31, 32]. Ambient temperature was measured using Raygner 3i handheld laser pyrometer at three different heights of 1.5 m, 3 m and 4.5 m above the ground. At each height, the temperature was measured at 64 points. For this purpose, rectangular aluminum plates (300 mm **x** 300 mm) were attached to a metal bar at each height. The laser beam of the pyrometer was directed to each point and the temperature was recorded.

Velocity

Air velocity was measured at the same points as described above using a hot-wire anemometer [33]. In addition, air velocity through roof ventilators, doors, windows, and roof monitors was measured to calculate ventilation flow rates, which were then used as boundary conditions for CFD modeling.

Computational Fluid Dynamics (CFD)

In this study, the commercial CFD code Airpak 3.0 (Fluent Inc., Lebanon, NH, USA) was used for the simulations. Airpak uses FLUENT to solve the Navier-Stokes equations for the transport of mass, momentum, species, and energy when calculating laminar and turbulent flows [34, 35]. Turbulence of air flow in space is modeled using a number of turbulence models, of which the most commonly used models are the zero-equation turbulence model, the k-ε turbulence model, and the Reynolds stress model [36]. Among these models, the k-ε turbulence model is the most widely used and popular turbulence model for simulating airflow in a space [37, 38]. The k-ε turbulence model is based on a transport equation for the turbulent kinetic energy k and a transport equation for the dissipation of the turbulent kinetic energy ε [39]. The standard k-ε turbulence model provides stable results and is suitable for general flow calculations, so, it was used for the simulations in this study. The CFD model was used to simulate the steady-state internal temperature and velocity during the application of different heat reduction strategies [40]. The convective heat transfer modeling in the k-ε models using the concept of Reynolds' analogy to turbulent momentum transfer is given by the following equation.

$$\frac{\partial}{\partial t}(\rho E) + \frac{\partial}{\partial x_i}[u_i(\rho E + p)] = \frac{\partial}{\partial x_i}\left(k_{eff}\frac{\partial T}{\partial x_i}\right) + S_h \quad (1)$$

Where ρ is the density, E is the total energy, t is the time, u_i is the summation of the mean and instantaneous velocity components (i = 1,2,3…), p is the pressure, k_{eff} is the effective conductivity, T is the temperature, and S_h is the volumetric heat source.

For the standard k-ε model, k_{eff} is given by

$$k_{eff} = k + \frac{c_p u_t}{Pr_t} \quad (2)$$

Where k is the conductivity of the material, C_p is the specific heat, U_t is the turbulent viscosity, and the default value of the turbulent Prandtl number (Pr_t) set to 0.85 [41].

In Airpak, the computational domain is first divided into discrete control volumes, followed by integration of the equations for each control volume to establish algebraic equations, which are later converted to linear equations and solved. Since Airpak is a commercial CFD code, its ability to simulate the temperature variations in the building had to be verified. To verify the CFD code, a grid dependence study was performed to ensure the convergence, consistency and stability of the CFD code [42]. An automatic hexa-unstructured grid from existing settings in Airpak was employed, which provided an accurate representation of the boundaries. An unstructured grid was used because it minimizes numerical error and provides a consistent solution across the modeling domain [43, 44]. Initially, a coarse grid was used, which was refined until the temperature values inside the building did not change significantly. In this study, the grid density was considered sufficient if the difference in average temperature at each elevation between successive denser grids was less than 5%.

Initial and boundary conditions

The geometry of the building and internal components used in the calculations of CFD is approximately the same as the original geometry of the building. The internal temperature during the measurement was approximately 33°C, which was used as the initial internal temperature during the simulation. The values of heat generated by each heat process were equated to the measured surface temperatures of each heat process. Air intake was through the southwest and south doors and air exhaust was through the north doors and other ventilation measures. The measured capacity of the exhaust air was about 3500 CMM and that of the supply air was about 2500 CMM at the same time. Hence, the air velocities at the inlet and outlet doors and ventilation measures were set to match the resulting airflow of 3500 CMM and 2500 CMM, respectively. The dimensions of the ventilation measures, the initial conditions and boundary conditions of the heat sources and the building are given in Table 1, Table 2 and Table 3, respectively.

Validation of the CFD model

The average measured and simulated temperature at 1.5 m, 3 m and 4.5 m above the ground, when all ventilation devices were open, was used to validate the CFD model. Three of the six criteria recommended by ASTM D 5157-96 were used for validation. The criteria used were: (1) correlation coefficient of 0.9 or higher, (2) regression slope between 0.75 and 1.25, and (3) regression intercept 25% or less of measured average temperature.

Table 1 Number and specification of existing ventilation measures

Serial Number	Description	Dimensions (in meter) (L x W x H)	Quantity
1	Door	4 x 0 x 3.5	1
2	Door	3.5 x 0 x 3.5	1
3	Door	3 x 0 x 3	1
4	Door	4 x 0 x 4	1
5	Door	3 x 0 x 3	1
6	Door	2 x 0 x 2.5	1
7	Roof ventilation monitor	32 x 2 x 2	1
8	Roof ventilation monitor	32 x 2 x 2	1
9	Opening	1 x 0 x 1	10
10	Roof fan	1 x 0 x 1	28

Table 2 Initial conditions for numerical modeling

Parameter	Values
Plant size	120 m x 84 m x 12 m
Ambient temperature	33° C
Exhaust ventilation volume	3550 m^3/min
Inlet volume	2500 m^3/min
Gravity vector	-9.8 m/s^2
Turbulent model	k-ε model
Time variation	Steady state
Variables solved	Temperature, Flow
Door status	Open

Table 3 Dimensions and properties of all heat sources in the building

Heat sources	Dimensions (in meter) (L x W x H)	Heat values		
		Front (°C)	Center (°C)	Back (°C)
HP 1	46 x 2 x 2	70	45	33
HP 2	49.5 x 2 x 2	70	45	33
HP 3	41 x 2 x 2	70	45	33
HP 4	13 x 2 x 2	40	50	50
HP 5a	4.5 x 2 x 3.5	54	52	48
HP 5b	4.5 x 2 x 3.5	58	56	53
HP 5c	4.5 x 2 x 3.5	58	58	53
HP 5d	19 x 2.5 x 5	80	75	70

Adjustments to the existing building

In order to reduce the existing temperature, several adjustments were made to the existing building by adding thermal control measures. The added components were:

Insulated Enclosures

The inspection of the heat sources revealed that the high temperatures inside the building were mainly due to the heat transfer from the heat sources and the inability of the insulation to control the existing heat transfer from the source to the room. To control the heat from the source, insulated partitions were installed at each of the heat sources [45]. Because frequent access to the heat source elements was required, the insulated partitions were installed 2 m above the floor and 1 m outside the surface of the heat sources. Most of the heated air would be trapped in the enclosure, as large amounts of heat would be released from the top of the heat source and hot air would be naturally forced up from the sides. The diagram of the insulated enclosure is shown in Figure 2.

Gravity Ventilators

The existing ventilators were installed along the length of the building, parallel to the wind direction. They were inefficient in removing the indoor air as they were not able to pull the hot air out of the building [46]. To solve this problem, a pair of ventilators with dimensions 40 m (L) **x** 2 m (W) **x** 2 m (H) were installed on both sides of the existing ventilators and placed directly above the insulated enclosures. The diagram of installed gravity ventilators is shown in Figure 2.

Windows

There were too few windows in the existing building, which was one of the major causes of the low airflow velocity inside the building and the lack of air pressure to direct the hot air through the exiting exits. More importantly, there were no windows on the southwest side of the building, the prevailing wind direction. These deficiencies were addressed by installing windows on the downwind side of the building along the entire length of the wall. The windows were installed in the upper part of the building, as this was where most of the hot air accumulated. Similarly, a total of 5 sets of windows were installed on the right and left sides of the building. The location and dimensions of the windows are shown in Figure 3.

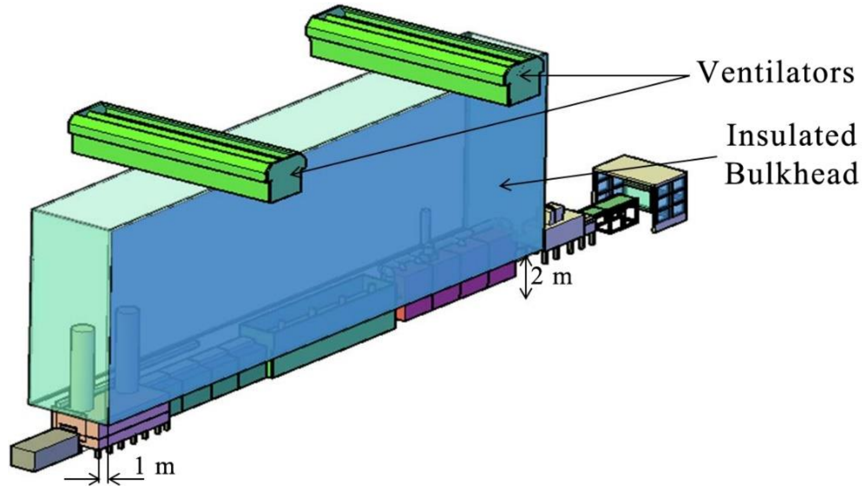

Figure 2 Diagram of insulated enclosures and gravity ventilators installed above heat sources 1-3

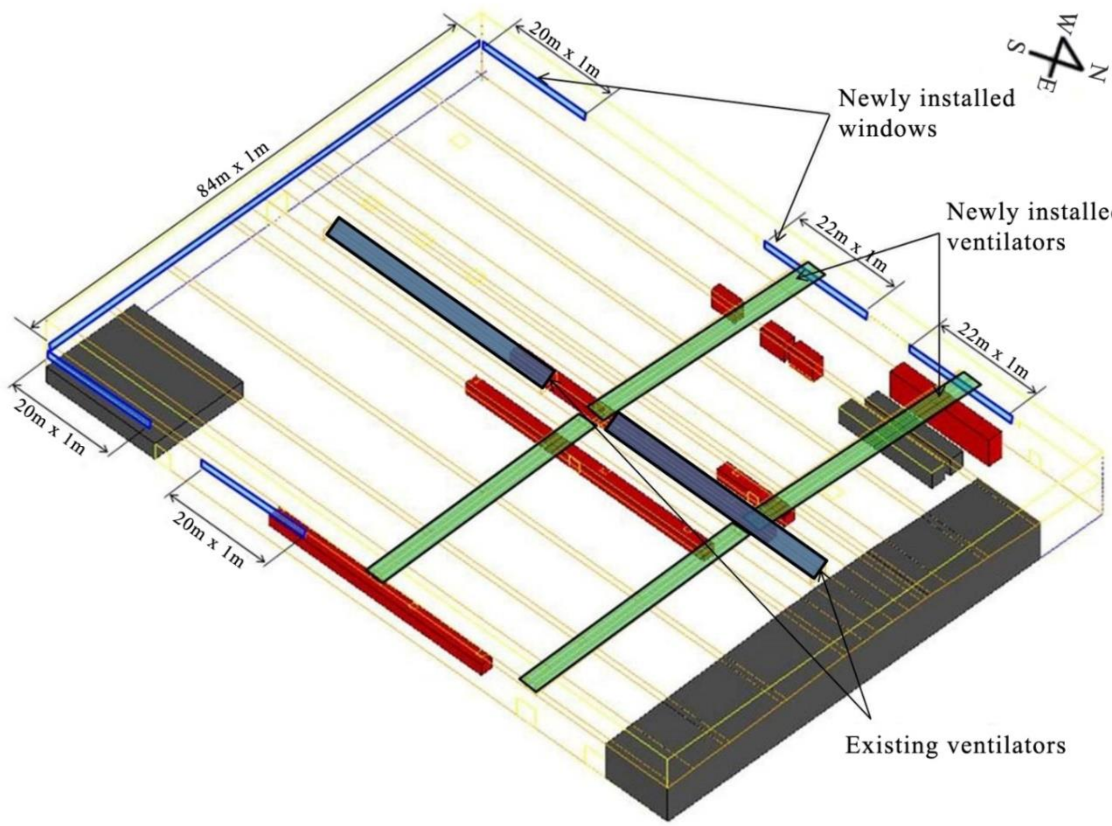

Figure 3 Diagram of building with newly installed gravity ventilators and windows

Jet Fans

Since the existing ventilation system was not able to generate the required air velocity, jet fans were considered as a possible solution [47]. Jet fans would improve the situation by maintaining a constant supply of air at high velocity, which was not the case with the existing ventilation. Jet fans could be placed in key areas where workers spend longer periods of time. The placement of jet fans took into consideration the obstructions created by various heat processes, some equipment in the building, and the position of the workers. Two types of jet fans (single jet fans and power jet fans) were used (their specifications are given in Table 4). The power jet fans were installed in the main aisles as shown in Figure 4. Single jet fans were used in conjunction with air conditioners to move cold air from the air conditioners at high velocity.

Table 4 Specifications of jet fans

Species	Specifications	
	Single jet fan	Power jet fan
Airflow (CMH)	600-2280	15000
Air speed (m/s)	10-25	33
Entrainment ratio	More than 25 times	More than 25 times
Power	0.38 kW/1 ϕ 220 V	5.5 kW/3 ϕ 440 V
Range	30 m/0.4 ms^{-1}	80 m/0.4 ms^{-1}

Installation of Air Conditioning Systems

In addition to the ventilation measures, air conditioning was installed to further reduce the temperature. The air-conditioning ducts were distributed along the areas of high heat generation and the outlets of the ducts were connected to single jet fans. The locations of the combination of air conditioning ducts and single jet fans are shown in Figure 4.

These components were used either individually or in combination to form six different cases as described in Table 5. Highest priority was given to natural ventilation and natural heat removal from the building, such as windows, enclosures, and ventilators. Case 1 was a model of existing conditions in the building. Windows and ventilators were added to Case 1 to create Case 2. Enclosing all heat sources in Case 2 resulted in Case 3. Power jet fans were added to Case 2 and Case 3 to develop Case 4 and Case 5, respectively. Similarly, air conditioners in conjunction with single jet fans were added to Case 5 to compose Case 6. A total of six cases were prepared and a CFD simulation was performed for each case. Temperature and velocity were predicted at a height of 1.5 m, 3 m and 4.5 m from the ground.

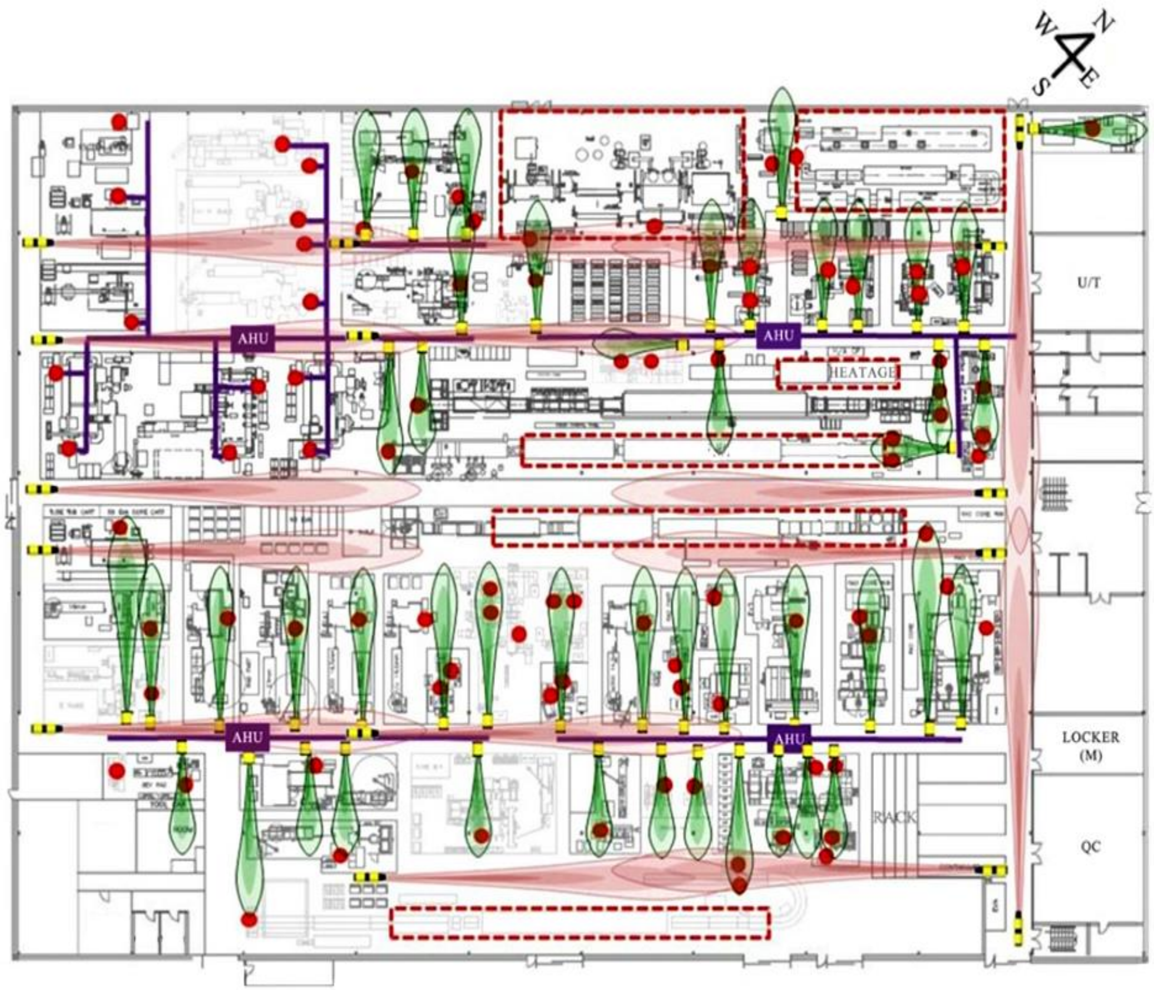

Figure 4 Position of workers (red dots) and planned installation positions of single jet fans (yellow blocks connected to green contours representing wind direction), power jet fans (double yellow blocks connected to red contours representing wind direction), and air conditioning (purple lines)

Table 5 Cases formed for CFD simulation

Cases	Installation of					Remarks	Number of grids in million (approx.)
	Windows	Ventilator	Enclosure in HP 1-5	Jet Fans	Air conditioners		
1	-	-	-	-	-	Original status	0.8
2	√	√	-	-	-	-	0.9
3	√	√	√	-	-	-	0.9
4	√	√	-	√	-	Power jet fans only	1.2
5	√	√	√	√	-	Power jet fans only	1.2
6	√	√	√	√	√	Power + single jet fans	1.2

Results and Discussion

Validation results of the CFD model

The average measured and simulated temperature as the preliminary test is shown in Figure 5. The regression curve and regression equation obtained by comparing the simulated and measured average temperature are shown in Figure 6. It shows that the correlation coefficient is 0.89 which is almost equal to the recommended criterion of 0.9, the slope of the regression is 0.83 which is between the recommended criteria of 0.75 and 1.25, and the intercept of the regression is 5.35 which is less than 25% of the measured average temperature. Therefore, it was considered that the CFD model is sufficiently able to model the temperature inside the building.

Case-based simulation results

The temperatures and air velocities predicted by CFC are listed in Table 6. Together with the predicted values, the distribution of temperature and air velocity at 1.5 m height is shown in Figure 7. The average ambient temperature during all experiments was 33°C. In case 1, representing the current condition of the building, the average temperature was 37.4°C, which was 4.4°C higher than the ambient temperature. The average air velocity was 0.12 m/s. The temperature was evenly distributed in the building and there was difficulty in removing the heat through the existing ventilation and ensuring adequate air velocity. The result is a lot of heat inside the building, which has a negative impact on the health of the workers and the productivity of the industry [7, 8].

As a first step towards improvement, windows and ventilators were installed in the CFD model (Case 2). This improvement had a direct effect on temperature as the average temperature dropped to 33.8°C, a decrease of 3.6°C. However, the air velocity did not increase significantly. The installation of enclosures on all heat sources (Case 3) resulted in a further 1.0°C decrease in temperatures, but the enclosure walls obstructed air flow and thus decreased air velocity. In Case 4, the enclosures were removed and power jet fans were installed in all aisles, near the heat sources. Compared to Case 2, this did not reduce the temperature as much, although the air velocity increased significantly. Moreover, the temperature in the areas near the heat sources where workers stay for long periods of time was 37.0°C, which is not desirable. As a result, both enclosures and power jet fans were added to Case 5. This helped to both lower the temperature and increase the air velocity; the resulting average temperature and air velocity were 33.2°C and 0.49 m/s, respectively. This is a significant decrease in temperature (5.2°C) and increase in air velocity (0.37 m/s) compared to Case 1. The final improvement involved air conditioning combined with single jet fans (Case 6). This configuration lowered the temperature to 32.0°C and increased the velocity to 0.82 m/s.

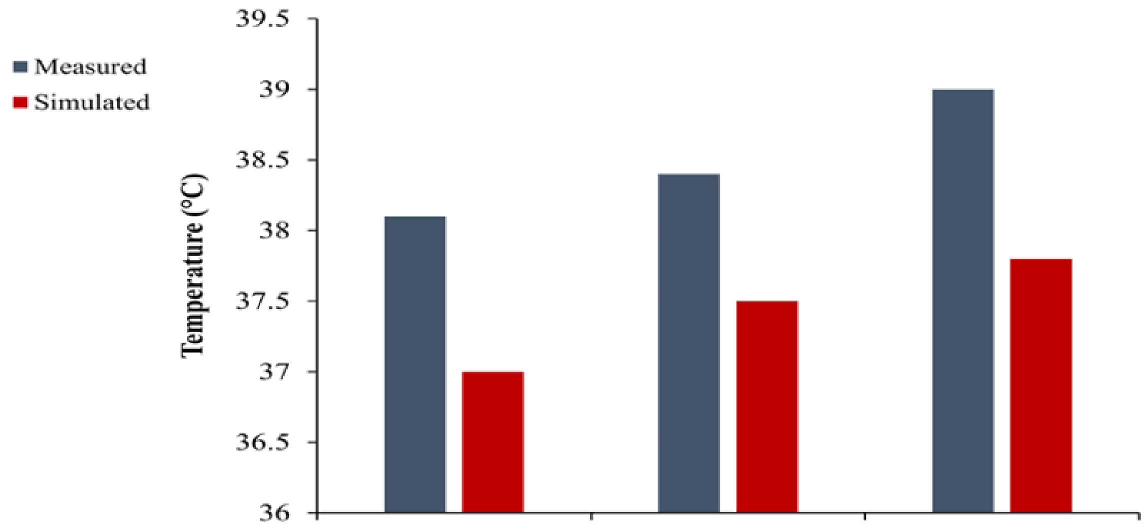

Height		1.5 m	3.0 m	4.5 m
Measured	Mean	38.1	38.4	39.0
	S.D.	3.02	2.93	3.34
Simulated	Mean	37.0	37.5	37.8
	S.D.	3.23	2.87	2.99

Figure 5 Comparison of average measured and simulated temperature at different heights

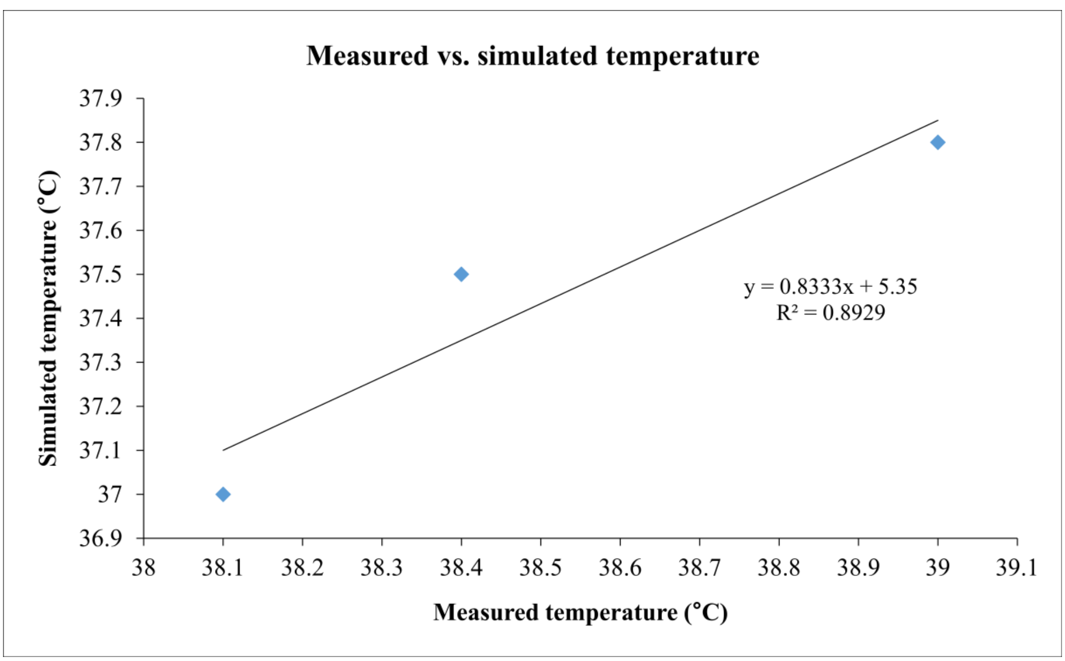

Figure 6 Simulated vs. measured temperature at all measurement heights

Table 6 CFD results of temperature and velocity

Cases	Temperature (°C)				Velocity (m/s)			
	1.5 m	3 m	4.5 m	Average	1.5 m	3 m	4.5 m	Average
1	37.0	37.5	37.8	37.4	0.14	0.11	0.10	0.12
2	33.6	33.8	34.1	33.8	0.18	0.12	0.09	0.13
3	33.2	33.3	33.4	33.3	0.09	0.07	0.06	0.07
4	33.5	33.5	33.6	33.5	0.40	0.45	0.77	0.54
5	33.2	33.2	33.3	33.2	0.34	0.40	0.72	0.49
6	31.9	32.0	32.0	32.0	0.73	0.74	0.99	0.82

Air conditioners are often the top energy-consuming parts in industrial plants [48]. Although the ventilation performance of Case 6 was the best; the cost of installation, operation and maintenance of the air conditioning system was expensive and the improvement in indoor conditions achieved in Case 6 was not much higher than that of Case 5. In Case 5, the temperature of 33.2°C was in the defined comfort zone of many studies [49-51] and a wind speed of 0.49 m/s was at a modest level that can help to provide better comfort. In Case 6, wind speeds in many areas of the work area were also above the appropriate level (< 1 m/s approximately) [52, 53]. Too high wind speed can cause adverse health effect to workers such as higher dust concentration in the air [54], higher noise level [55], dry eyes [56], and so on. Thus, Case 5 was adopted as the optimal case for application in the existing industry.

Application to the Real Site

The solution selected from the simulation results of CFD, Case 5, was applied to the existing building to measure its effectiveness and performance in the real world. All the components i.e. windows, ventilators, enclosures, and jet fans were installed in the building. Extra care was taken to ensure that the real installations matched the CFD model as faithfully as possible. The real temperature and velocity measurements are shown in Table 7. There is a good correlation between the Case 5 results predicted by CFD and the experimental results; the difference between the results at 1.5 m, 3 m, and 4.5 m was 1.8%, 2.7%, and 3.3%, respectively. The temperatures and air velocities of the original and improved building setups are compared in Figures 8 and 9. The provided ventilation solution was able to reduce the average temperature by 5.3° C and increase the average air velocity by 1.5 m/s.

However, aforementioned discussion is only a matter of success in lowering the temperature, but it is the initial fundamental factor that must be considered [48]. Although the operators were satisfied with the current conditions in the work area after the improvement, another point that should be further observed in the long term is the comfort of each operator due to the different wind speeds in locations which is subjective [57]. Maintaining air flow uniformity is always not easy when a jet fan is the chosen option for industrial ventilation [58].

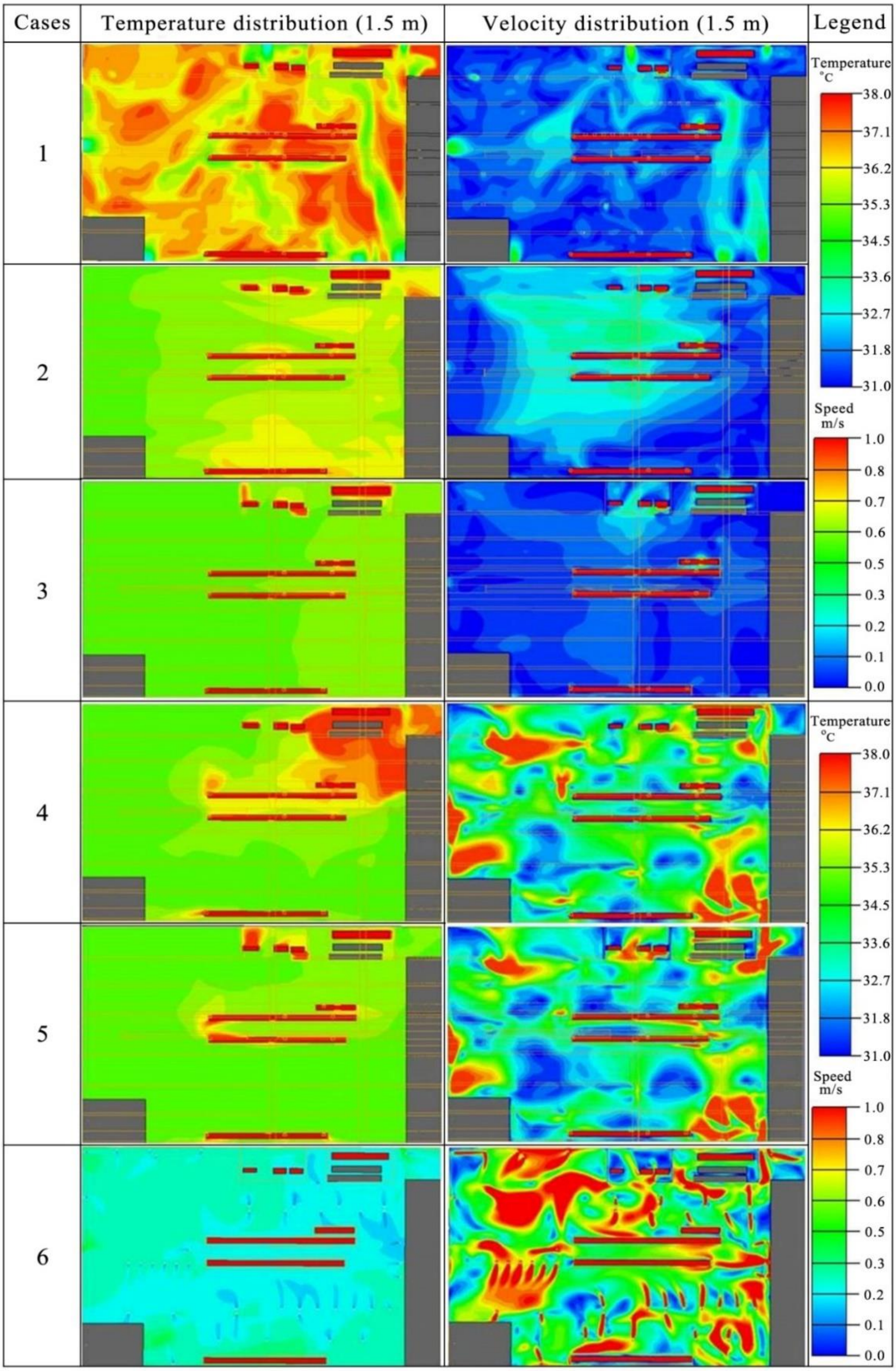

Figure 7 CFD-predicted results of temperature and air velocity distribution

Table 7 Comparison of CFD simulated and measured temperature for improved condition (Case 5)

Height (m)	CFD simulated temperature (°C)	Measured temperature (°C)	Difference (%)
1.5	33.2	33.8	1.80
3	33.2	34.1	2.70
4.5	33.3	34.4	3.33

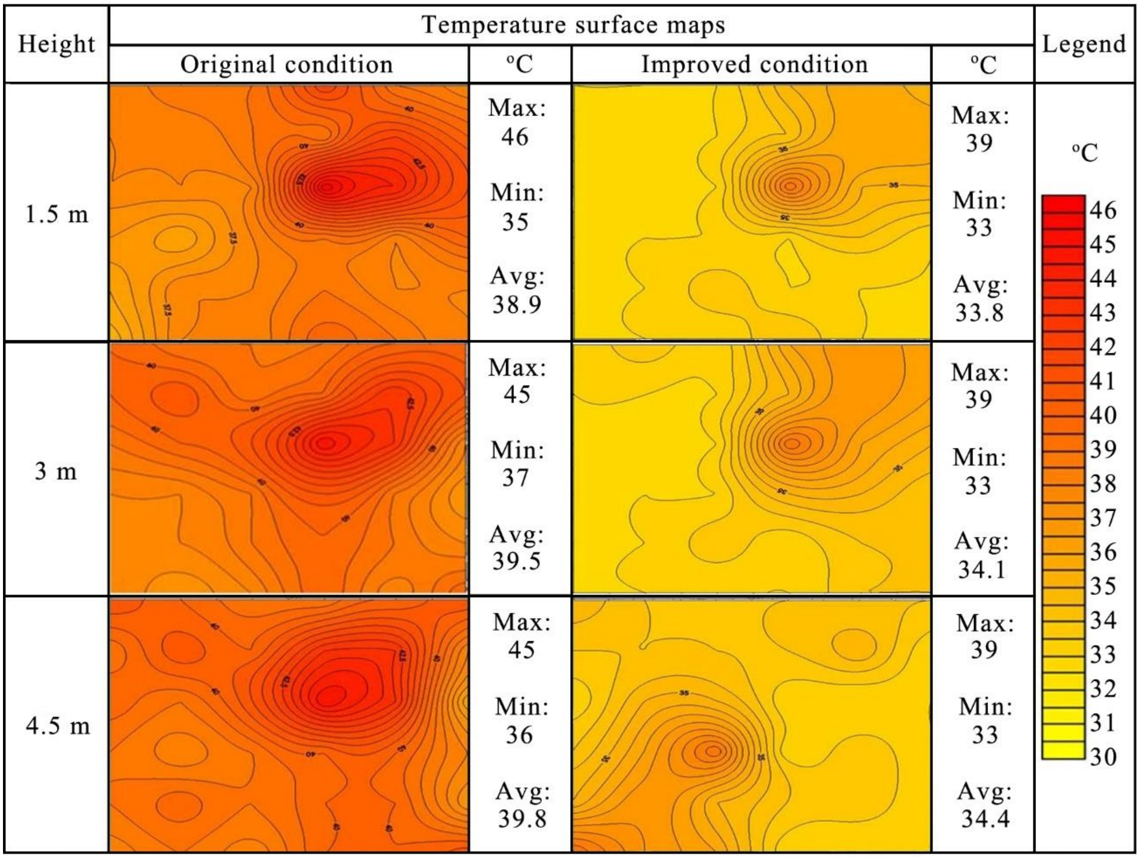

Figure 8 Comparison of temperature between original and improved conditions

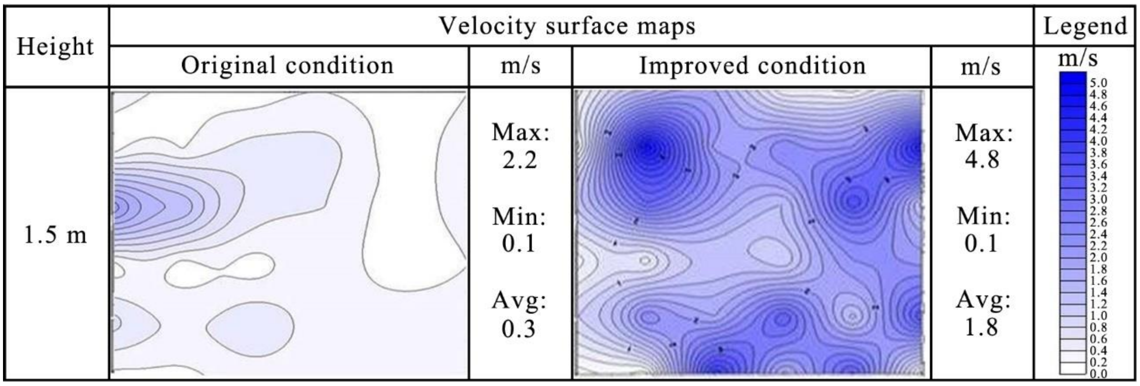

Figure 9 Comparison of air velocity between original and improved conditions

Conclusions

This research is an attempt to solve the problem of high temperatures in an existing industrial workshop environment. Although general and local exhaust ventilations have been a topic of extensive research on the elimination of gases and pollutants in the workplace, these methods may not be effective for heat-related problems. This paper provides some insight into the application of various techniques. In addition to the obvious heat control options, jet fans have been used as a potential solution because they can supply a constant flow of air at high velocity.

The research is accomplished through the successive use of experimental and numerical methods. Firstly, the problem was identified by measuring the related factors and then understanding the possible solutions that could be implemented. The effectiveness of the possible solutions is examined by using CFD simulations. The optimal option (reaching maximum temperature for acceptability with an appropriate level of wind movement) identified by CFD is implemented in the real site. Ventilation designs presented in this study can be an example that helps inspire the factory manager to consider other innovative options apart from air conditioners usually installed against high workplace temperatures (with a high cost of energy consumption). From the results of the final application in the real site, it is found that the installed system was able to dissipate sufficient amounts of heat and make the workplace comfortable for the workers with no complaints.

Although this study still leaves some questions unanswered, such as the comparison of the final conditions in the building with the available standards and limits, the use of air conditioning in the real application, these limitations are mainly due to a lack of resources. This presents a good opportunity for further investigation into different ventilation options for workplace heat control and comparison with standard limits. Nevertheless, the analysis of ventilation and the methods provided by this research should help to make the workplace more comfortable and safer.

Acknowledgements

This research was conducted with financial support from Changwon National University, South Korea, and with the sponsorship from the National Research Council of Thailand (NRCT) – the National Research Foundation of Korea (NRF) Scientist Exchange Program 2021.

References

[1] Wiriyasart, S. and Naphon, P. 2019. Numerical study on air ventilation in the workshop room with multiple heat sources. Case Studies in Thermal Engineering. 13, 100405: 1-11.

[2] Akhtar, M., Qamar, S.Z., Muhammad, M. and Nadeem, A. 2018. Optimum heat treatment of aluminum alloy used in manufacturing of automotive piston components. Materials and Manufacturing Processes. 33(16): 1874-1880.

[3] Edenhofer, B., Lankes, H.P., Burgmaier, H. and Kurz, A. 2013. The flexible heat treatment of automotive components in a novel type of pusher furnace. La Metallurgia Italiana. 98(2): 39-45.

[4] Qu, S. and Gong, Y. 2021. Effect of heat treatment on microstructure and mechanical characteristics of 316L stainless steel parts fabricated by hybrid additive and subtractive process. The International Journal of Advanced Manufacturing Technology. 117(11): 3465-3475.

[5] Gladshtein, V.I. and Lyubimov, A.A. 2021. Selection Criteria for Heat Treatment in Order to Optimize Reconstructed Heat Supply Turbine Body Metal Component Properties. Power Technology and Engineering. 54(6): 896-903.

[6] Kong, D., Ni, X., Dong, C., Zhang, L., Man, C., Yao., J., Xiao, K. and Li, X. 2018. Heat treatment effect on the microstructure and corrosion behavior of 316L stainless steel fabricated by selective laser melting for proton exchange membrane fuel cells. Electrochimica Acta. 276: 293-303.

[7] Ciuha, U., Pogacar, T., Bogataj, L.K., Gliha, M., Nybo, L., Flouris, A.D. and Mekjavic, I.B. 2019. Interaction between Indoor Occupational Heat Stress and Environmental Temperature Elevations during Heat Waves. Weather, Climate, and Society. 11: 755-762.

[8] Chowdhury, S., Hamada, Y. and Ahmed, S. 2017. Indoor heat stress and cooling energy comparison between green roof (GR) and non-green roof (n-GR) by simulations for labor intensive factories in the tropics. International Journal of Sustainable Built Environment. 6(2): 449-462.

[9] Pogačar, T., Casanueva, A., Kozjek, K., Ciuha, U., Mekjavić, I.B., Bogataj, L.K. and Črepinšek, Z. 2018. The effect of hot days on occupational heat stress in the manufacturing industry: implications for workers' well-being and productivity. International Journal of Biometeorology. 62(7): 1251-1264.

[10] Nerbass, F.B., Pecoits-Filho, R., Clark, W.F., Sontrop, J.M., McIntyre, C.W. and Moist, L. 2017. Occupational Heat Stress and Kidney Health: From Farms to Factories. Kidney International Reports. 2(6): 998-1008.

[11] OSHA Technical Manual. 2015. Section III: Chapter 4.

[12] Morrissey, M.C., et al. 2021. Heat Safety in the Workplace: Modified Delphi Consensus to Establish Strategies and Resources to Protect the US Workers. GeoHealth. 5(8): 1-32.

[13] Yin, M., Hu, H., We, K., Wei, Y., Zhang, X., Zhu, K. and Yan, X. 2021. Computational study on effects of jet fans to traffic force in highway tunnel. Tunnelling and Underground Space Technology. 118, 104155: 1-14.

[14] Nazari, A., Jafari, M., Rezaei, N., Taghizadeh-Hesary, F. and Taghizadeh-Hesary, F. 2021. Jet fans in the underground car parking areas and virus transmission. Physics of fluids. 33(1), 013603: 1-12.

[15] Senveli, A., Dizman,T., Celen, A., Bilge, D., Dalkılıç, AS. and Wongwises, S. 2015. CFD Analysis of Smoke and Temperature Control System of an Indoor Parking Lot with Jet Fans. Journal of Thermal Engineering. 1(2): 116-130.

[16] Weisenpacher, P. and Valasek, L., Computer simulation of airflows generated by jet fans in real road tunnel by parallel version of FDS 6. 2021. International Journal of Ventilation. 20(1): 20-33.

[17] Weng, M., Obadi, I., Wang, F., Liu, F. and Liao, C. 2020. Optimal distance between jet fans used to extinguish metropolitan tunnel fires: A case study using fire dynamic simulator modeling. Tunnelling and Underground Space Technology. 95, 103116: 1-12.

[18] Çakir, M.T. and Ün, Ç., CFD Analysis of Smoke and Temperature Control System of Car Park Area with Jet Fans. 2020. Journal of Engineering Research and Reports. 13(3): 27-40.

[19] Sultansu, S. and Onat, A. 2020. The CFD Analysis of Ventilation and Smoke Control System with Jet Fan in a Parking Garage. International Journal of Advances in Engineering and Pure Sciences. 32(1): 89-95.

[20] Sverdlov, A.V., Volkov, A.P., Volkov, M.A. Rykov, S.V. and Guliyants, M.M. 2020. Increasing energy efficiency and resource saving thanks to the design solution on the use of reversible jet ventilation system for four-storied underground garage in national cultural center of Kazan. Journal of Physics: Conference Series. 1565, 012085: 1-6.

[21] Nielsen, P.V. 2004. Computational fluid dynamics and room air movement. Indoor Air. 14(s7): 134-143.

[22] Cao, S.J. 2019. Challenges of using CFD simulation for the design and online control of ventilation systems. Indoor and Built Environment. 28(1): 3-6.

[23] Shen, P. and Wang, Z. 2020. How neighborhood form influences building energy use in winter design condition: Case study of Chicago using CFD coupled simulation. Journal of Cleaner Production. 261, 121094: 1-19.

[24] Zhang, X., Weerasuriya, A.U. and Tse, K.T. 2020. CFD simulation of natural

ventilation of a generic building in various incident wind directions: Comparison of turbulence modelling, evaluation methods, and ventilation mechanisms. Energy and Buildings. 229, 110516: 1-19.

[25] Prakash, D. 2015. Transient analysis and improvement of indoor thermal comfort for an air-conditioned room with thermal insulations. Ain Shams Engineering Journal. 6(3): 947-956.

[26] Alwetaishi, M. and Gadi, M. 2021. New and innovative wind catcher designs to improve indoor air quality in buildings. Energy and Built Environment. 2(4): 337-344.

[27] Gilani, S., Montazeri, H. and Blocken, B. 2016. CFD simulation of stratified indoor environment in displacement ventilation: Validation and sensitivity analysis. Building and Environment. 95: 299-313.

[28] Heidarinejad, G., Fathollahzadeh, M.H. and Pasdarshahri, H. 2015. Effects of return air vent height on energy consumption, thermal comfort conditions and indoor air quality in an under floor air distribution system. Energy and Buildings. 97: 155-161.

[29] Chen, Z., Xin, J. and Liu, P. 2020. Air quality and thermal comfort analysis of kitchen environment with CFD simulation and experimental calibration. Building and Environment. 172, 106691: 1-11.

[30] Woodson, R.D. 2012. Chapter 8 - OSHA Regulations, in Construction Hazardous Materials Compliance Guide, Woodson, R.D. Editor. Butterworth-Heinemann: Boston. 115-143.

[31] Bembenek, M. and Uhrynski, A. 2021. Analysis of the Temperature Distribution on the Surface of Saddle-Shaped Briquettes Consolidated in the Roller Press. Materials. 14(7), 1770: 1-16.

[32] Usamentiaga, R., Venegas, P., Guerediaga, J., Vega, L., Molleda, J. and Bulnes, F.G. 2014. Infrared thermography for temperature measurement and non-destructive testing. Sensors. 14(7): 12305-12348.

[33] Thollander, P., Karlsson, M., Rohdin, P., Wollin, J. and Rosenqvist, J. 2020. Introduction to Industrial Energy Efficiency. Cambridge, UK: Academic Press.

[34] Hoult, R.E. and Kovtun, P. 2020. Stable and causal relativistic Navier-Stokes equations. Journal of High Energy Physics. 67: 1-14.

[35] Tao, T. 2019. Searching for singularities in the Navier–Stokes equations. Nature Reviews Physics. 1(7): 418-419.

[36] Joshi, J.B., et al. 2019 Computational fluid dynamics, in Advances of Computational Fluid Dynamics in Nuclear Reactor Design and Safety Assessment, Joshi J.B. and Nayak A.K. Editors., Woodhead Publishing. 21-238.

[37] Mularski, J., Arora, A., Saeed, M.A., Niedzwiecki, L. and Saeidi, S. 2020. Impact of Turbulence Models on the Air Flow in a Confined Rectangular Space. Engineering Science & Technology. 2(1): 46-53.

[38] Gunadi, G.G., Siswantara, A.I., Budiarso, B., Daryus, A. and Pujowidodoet, H. 2016. Turbulence Model and Validation of Air Flow in Wind Tunnel. International Journal of Technology. 8: 1362-1372.

[39] Baukal Jr., C.E., 2013. The John Zink Hamworthy Combustion Handbook: Three-Volume Set. Boca Raton, Florida: CRC Press.

[40] Fatima, S.F. and Chaudhry, H.N. 2017. Steady-state CFD modelling and experimental analysis of the local microclimate in Dubai (UAE). Sustainable Building. 2(5): 1-12.

[41] Fluent Inc. 2007. AIRPAK 3.0 user's guide. Centerra Resource Park, Lebanon.

[42] Tu, J., Inthavong, K. and Ahmadi, G. 2012. Computational Fluid and Particle Dynamics (CFPD): An Introduction. Computational Fluid and Particle Dynamics in the Human Respiratory System, Springer, Dordrecht: 1-18.

[43] Yang, X., An, W., Li, W. and Zhang, S. 2020. Implementation of a Local Time Stepping Algorithm and Its Acceleration Effect on Two-Dimensional Hydrodynamic Models. Water. 12(4), 1148: 1-24.

[44] Thomas, J.L., Diskin, B. and Rumsey, C.L. 2008. Towards Verification of Unstructured-Grid Solvers. AIAA Journal. 46(12): 3070-3079.

[45] Zyczynska, A. 2014. The heat consumption and heating costs after the insulation of building partitions of building complex supplied by the local oil boiler room. Eksploatacja i Niezawodność. 16(2): 313-318.

[46] Ye, W., Zhang, X., Gao, J., Gao, G. Zhou, X. and Su, X. 2017. Indoor air pollutants, ventilation rate determinants and potential control strategies in Chinese dwellings: A literature review. Science of The Total Environment. 586: 696-729.

[47] Giesen, B.J.M.v.d., Penders, S.H.A., Loomans, M.G.L.C., Rutten, P.G.S. and Hensen, J.L.M. 2011. Modelling and simulation of a jet fan for controlled air flow in large enclosures. Environmental Modelling & Software. 26(2): 191-200.

[48] Chen, C., Lai, D. and Chen, Q. 2020. Energy analysis of three ventilation systems for a large machining plant. Energy and Buildings. 224, 110272: 1-11.

[49] Kumar, S., Mathur, J., Mathur, S., Singh M.K. and Loftness, V. 2016. An adaptive approach to define thermal comfort zones on psychrometric chart for naturally ventilated buildings in composite climate of India. Building and Environment. 109: 135-153.

[50] Pereira P.F.C.P. and Broday E.E. 2021. Determinaiton of thermal comfort zones through comparative analysis between different characterization methods of thermally dissatisfied people. Buildings. 11(320): 1-26.

[51] Srisuwan P. and Shoichi K. 2017. Field investigation on indoor thermal environment of a high-rise condominium in hot-humid climate of Bangkok, Thailand. Procedia Engineering. 180: 1754-1762.

[52] Esfahankalateh A.T., Farrokhzad M., Saberi O. and Ghaffarianhoseini A. 2021. Achieving wind comfort through window design in residential buidlings in cold climates, a case study in Tabirz city. International Journal of Low-Carbon Technologies. 16: 502-517.

[53] Givoni B. 1992. Comfort, climate analysis and buidling design guidelines. Energy and Buildings. 18: 11-23.

[54] Scibor M., Bokwa A. and Balcerzak B. 2020. Impact of wind speed and apartment ventilation on indoor concentrations of PM10 and PM2.5 in Krakow, Poland. Air Quality, Atmosphere & Health. 13: 553-562.

[55] King E., Mahon J. and Pilla F. 2009. Measuring noise in high wind speeds: evaluating the performance of wind shields. Inter-Noise, 23-26 August 2009, Ottawa, Canada.

[56] Davis J.A., Ousler G.W., Langelier N.A., Schindelar M.R., Abelson R. and Abelson M.B. 2006. Seasonal changes in dry eye symptomatology. Investigative Ophthalmology & Visual Science. 47, 280: 1.

[57] Zhou, B., Yang, B., Wu, M., Guo, Y., Wang, F. and Li, A. 2022. Draught sensation assessment in an occupied space heated by stratified ventilation system: Attachment ventilation with relayed fans. Building and Environment, 207, 108500: 1-12.

[58] Zhang, Y., Kacira, M. and An, L. 2016. A CFD study on improving air flow uniformity in indoor plant factory system. Biosystems Engineering. 147: 193-205.